Variance in TLM diffusion simulations

P. Chardaire and D. de Cogan[1]

Abstract

The excitation of TLM diffusion models has close similarities with statistical processes. A constant magnitude source yields an erfc profile, while the diffusion following a single-shot excitation looks very similar to a Gaussian distribution. The dependence of profile on TLM scattering parameters has been investigated by examining their effect on variance as a function of iteration time. Initially a brute-force analysis was used, but this has been supeceded by a formal proof of the relationship and has been extended to higher dimensions.

Introduction

Several years ago a TLM research project sought to devise a method of dynamic mesh expansion for heat-flow modelling. The feeling was that if heat came from a single source then there was little point in shifting zeros around an array. Instead, we sought to expand the mesh in front of the heat source. A BSc final year project at Nottingham University devised a scheme whereby the peripheral nodes around the mesh were monitored until their temperature rose above a preset value (e.g. 0.01ºC), at which point the entire matrix would be expanded by that amount. A subsequent final year project demonstrated the extent of computational saving that could be achieved by this means. Attempts to publicise these observations were unsuccessful, the reviewers commenting on the lack of any formal basis. For this reason we have spent much time examining the statistics of TLM models for Gaussian diffusion. The following is an edited extract from [1] with some annotation.

> A single-shot injection will lead to a Gaussian diffusion which will have a standard deviation, σ, which depends on the TLM reflection and transmission coefficients, ρ, τ and iteration time-step, k. The error due to the truncation of a Gaussian distribution at a given number of standard deviations is well known and it was felt that the relationship between σ, and the TLM parameters ρ,τ and k would constitute a better basis for mesh truncation.

---

[1] School of Information Systems, University of East Anglia, Norwich NR4 7TJ (UK)

This was approached using statistical analysis by Cox [2]. The first step involved an investigation of the conditions when the TLM simulation of single shot injection could be considered as a Gaussian distribution. analysis used a one-dimensional bar of material where the space and time discretisations were arranged so that the TLM model depended only on the reflection coefficient, ρ. A single pulse of magnitude equivalent to a temperature rise of 200°C was injected into the centre so that heat diffused symmetrically. Temperature profiles were collected after every iteration and were tested for normality using the Chi-square test. Figure 1 shows the Chi-square test probability plotted against iteration number, k for different values of ρ. If we accept a 95% confidence limit for the test, we may say that a profile is a normal distribution when the ordinate value in the figure is above 0.95. Hence, when $\rho = 0.5$, the distribution is normal after only 3 iterations but for $\rho = 0.1$, approximately 27 iterations are required before a normal distribution is reached. These tests showed no difference for profiles calculated using either link-resistor or link-line nodal configuration.

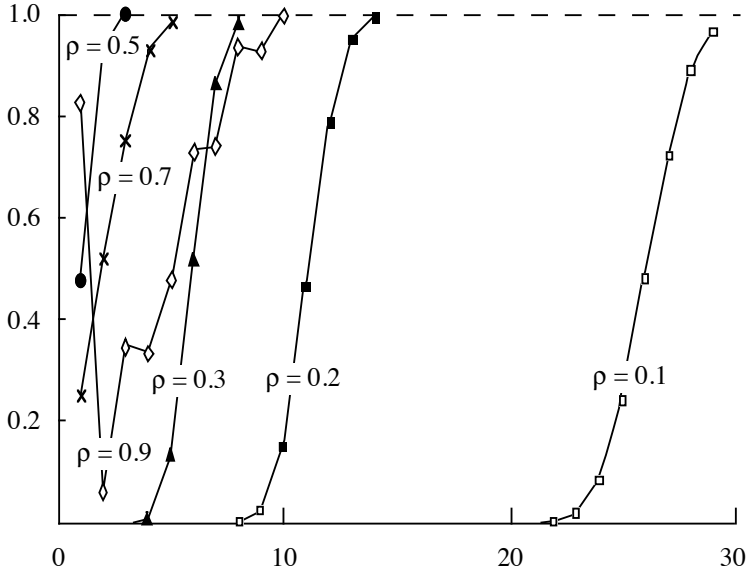

Figure 1 Significance of fit to a Gaussian distribution (vertical axis) versus number of iterations (horizontal axis) as a function of ρ for a single injection into an infinite one-dimensional sample.

The profile data was used to calculate variance (σ^2) which was then plotted against k (after convergence to normality) for different values of ρ. The dependence of the variance on *k* was found to be linear in all cases and straight lines were fitted to the points using a standard linear regression routine. The regression lines have the form $ak + b$ and 95% confidence intervals for the values of a were calculated. The largest confidence interval was 1.7×10^{-5} for $\rho = 0.1$. For $\rho = 0.5$, the confidence interval was zero i.e. the linear fit was perfect to within the numerical accuracy of the computer. Analysis of the dependence of σ^2 on ρ for the link-line node showed that:

$$_{LL}\sigma^2(k) = \frac{\tau}{\rho}k + \frac{1}{2} - \frac{\tau}{\rho}\left[1-\frac{\tau}{2\rho}\right] \qquad (1)$$

Even in one-dimensional diffusion models there are alternative network formulations and the distinction is shown in figure 2. They are effectively observations of the same material that are displaced by $\Delta x/2$ in space and $\Delta t/2$ in time and some of the consequences of choosing one or another formulation in a simulation are discussed in [3]

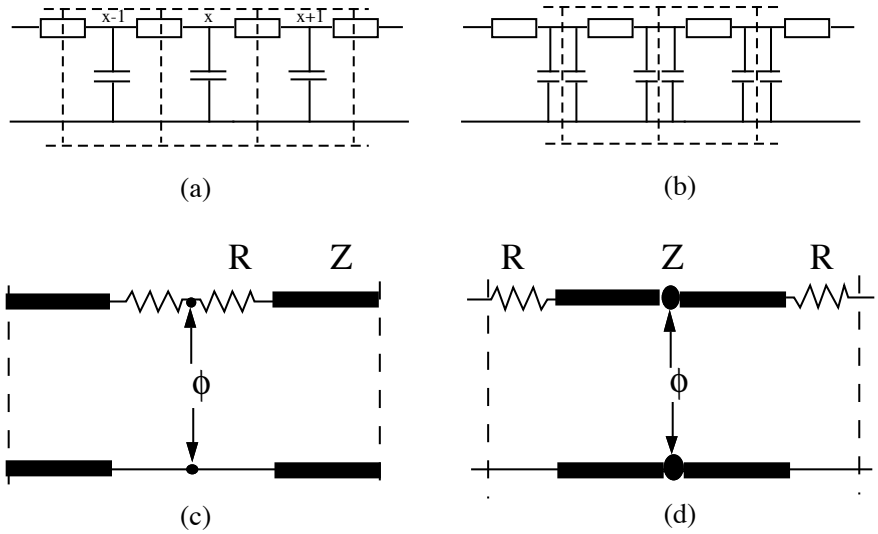

Figure 2 (a) T-network electrical analogue for diffusion, (b) Π-network analogue, (c) link-line TLM node, (d) link-resistor TLM node

The statistical analysis outlined above was for a link-line network. When a similar analysis was undertaken for a link-resistor network, it was found to be smaller by 0.5

$$ {}_{LR}\sigma^2(k) = \frac{\tau}{\rho}k - \frac{\tau}{\rho}\left[1-\frac{\tau}{2\rho}\right] \qquad (2) $$

The analytical expression for Gaussian diffusion gives a variance which is related to space, time and the diffusion constant, D. We can move to discretised space, $x \rightarrow n\Delta x$ and time, $t \rightarrow k\Delta t$ and relate D to the TLM scattering parameters. If we have unit spatial discretisation then it can be shown that

$$ \sigma^2 = \frac{\tau}{\rho}k \qquad (3) $$

It is believed that the additional terms in eqns (1) and (2) are a feature of the TLM approximation to the diffusion equation and researches involving Stephen Cox, Kimberly Moravec and others have sought to quantify these. This paper will start by explaining the 'sledge-hammer' approach that was used initially. It will then go on to outline the elegant method due to Chardaire [4] and will conclude with some comments on the extension to higher dimensions.

Binary scattering

The following is another edited extract [5]

> The diagram above shows the space-time history of a one-dimensional array of nodal points where a signal of unit magnitude (incident from the left) strikes position *x* and is scattered in the proportions ρ and τ (where $\rho + \tau = 1$). At the next time-step these are scattered (the scattering of a signal from the right being a mirror image of that for a pulse from the left). As scattering progresses we can see similarities with Pascal's triangle. For instance, we can see that at time k = 2 in the diagram above there are three components each of total power, 2. These comprise $\rho\tau$ at (x-2), $\rho\tau$ and ρ^2 at (x) and τ^2 at (x+1), i.e.in the ratio 1:2:1. At the next timestep these components are in the ratio 1:3:3:1. The only problem is that every point becomes the start point for a new Pascal triangle; there is self similarity and it not possible at first sight to predict the total population of any position at some time in the future.
>
> Much information on this can be obtained using simple shift-operators. As shown in the diagram above each contributor requires two description parameters, magnitude and direction of motion. These can be quantified by a reflection operator, $\hat{\rho}$ and a transmission operator $\hat{\tau}$
>
> $\hat{\rho}$ has two effects:
>
> It alters the pulse magnitude by a factor, ρ
>
> It reverses the direction of movement of a pulse, and shifts it by one position.
>
> Thus, if an input of unit magnitude, arriving at position x from the left is designated as (x), then
>
> $$\hat{\rho}(x) = \rho(x-1)$$
>
> If $\hat{\rho}$ acts on this then $\hat{\rho}\,\rho(x-1) = \rho^2(x-1+1)$ i.e. ρ^2
>
> This is the value at the origin, which is exactly what is observed in the diagram.

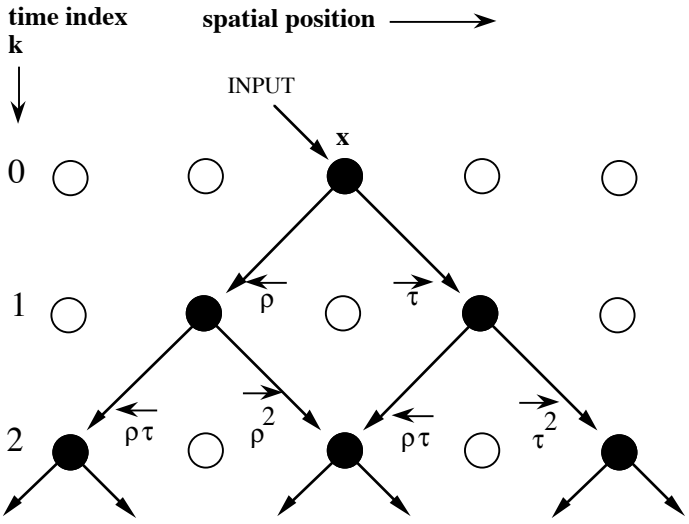

Figure 3 Scatter diagram for an initial input from the left

The transmission operator, $\hat{\tau}$ has two effects:

- It alters the pulse magnitude by a factor, τ
- It maintains the direction of movement of a pulse, and shifts it by one position.

For the pulse incident at location, x from the left we can write

$$\hat{\tau}(x) = \tau(x+1)$$

These operators are associative, but not commutative. It is quite clear from an inspection of figure 3 that the sequence of operations $\hat{\rho}\,\hat{\tau}$ and $\hat{\tau}\,\hat{\rho}$ have identical effects on the magnitude of a pulse, but they result in pulses with quite different final locations.

Within the scatter diagram we can also identify regions of influence and regions of dependence. Inspection of the figure 4a shows that the shaded region falls within a triangle whose apex constitutes a limit of influence.

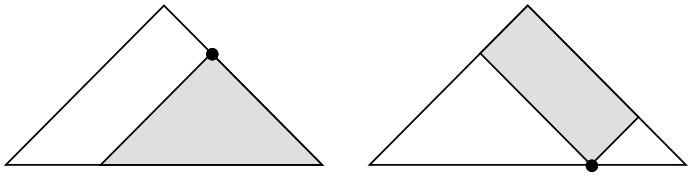

(a) (b)

Figure 4 (a) One-dimensional TLM/CRW scatter diagram with domain of influence of an individual point shown shaded. (b) domain of dependence of an individual point in a scatter diagram.

Similarly the point identified in figure 4 (b) is dependent only on the shaded region above it. The total population at any position at any time is the result of all paths which start at the origin and arrive by a sequence of all possible binary paths to the point (figure 5).

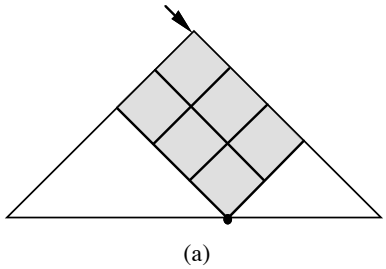

(a)

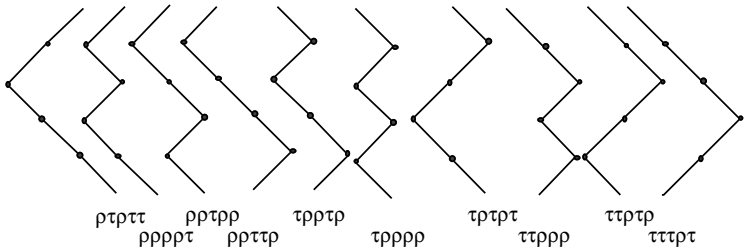

(b)

Figure 5 (a) The domain of dependence of the point (x+1) at time k = 5, (b) all possible paths which start at the origin and end at the point in question together with the reflection/transmission operations which are read from left to right.

Estimation of P(x,k)

We now use the concept of domain of dependence to estimate P(x,k) for a single injection from the left.

These are due to Chardaire and to Moravec. The Chardaire method, although slightly less universal in its application is simpler to understand and will be presented here. Details of the Moravec method can be found in [5].

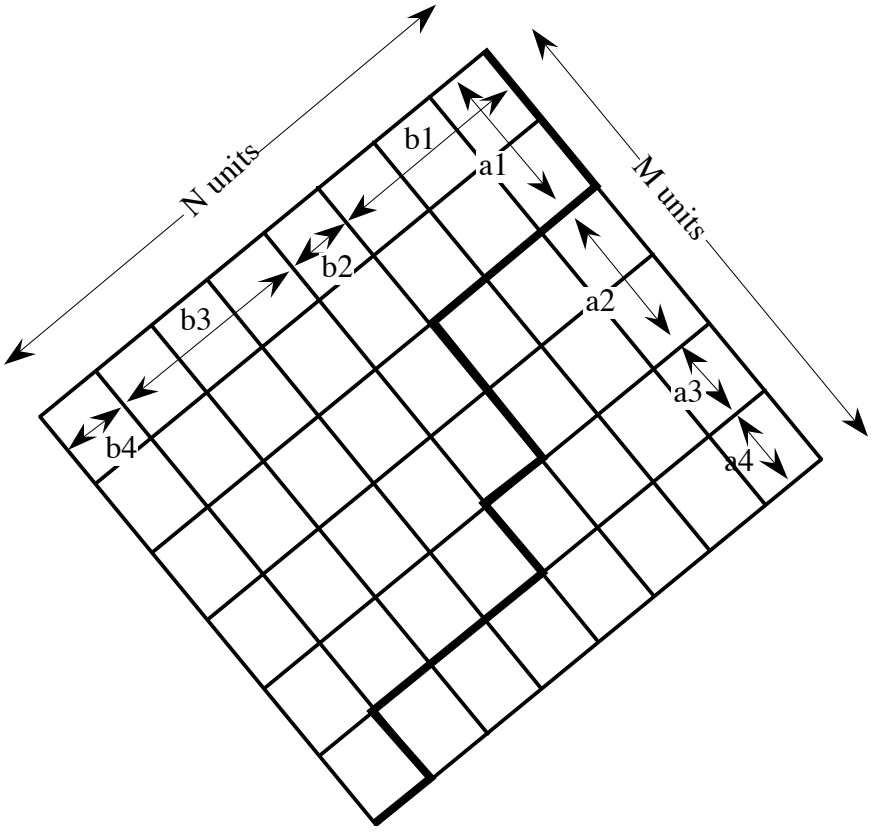

Figure 6 A sequence of seven turns that will have an expression of the form $A\rho^7\tau^7$.

It can that the situation in figure 6 could be arranged into a sequence: a_1, b_1, a_2, b_2, a_3, b_3, a_4, b_4. In a more general sense there could be *r* pairs $[a_1, b_1, a_2, b_2, \ldots, a_r, b_r]$ with (2r-1) changes. The question then is how can we arrange these with a_r changes in M-units and b_r changes in N-units? The result is:

$$\binom{M-1}{r-1}\binom{N-1}{r-1}\tau^k\left(\frac{\rho}{\tau}\right)^{2r-1} \qquad (4)$$

If this is done for every value of $r \leq \min(M,N)$ and for all values from M=1 to (k-1) with N = k-M we obtain all the possible contributions from this source. However, there are three other contributing sources.

In the case shown below there is a sequence: a_1, b_1, a_2, b_2, a_3 (r = 3). There are a total of four turnings. In more general terms this is a sequence: $[a_1, b_1, a_2, b_2, \ldots b_{r-1}, a_r]$ with (2r-2) changes.

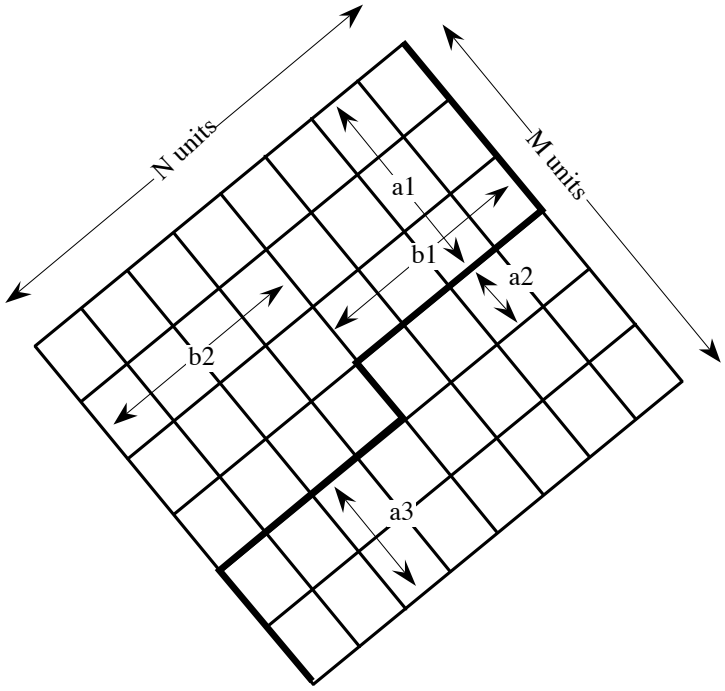

Figure 7

The permuations are:

$$\binom{M-1}{r-1}\binom{N-1}{r-2}\tau^k\left(\frac{\rho}{\tau}\right)^{2r-2} \qquad (5)$$

The constraint is that $r \leq \min(M, N+1)$

The two contributions above started with a_1, one or more transmission operations (i.e. the first progressed down the M-diagonal. The next two contributions start with one or more reflection operations and first progress down the N-diagonal.

The diagram in figure 8 has 6 changes with r = 3 in the sequence $b_1, a_1, b_2, a_2, b_3, a_3$ (remember that the entry point represents a turn, since we had incidence from the left). In general this is a sequence $[b_1, a_1, b_2, a_2, \ldots, b_r, a_r]$ with (2r) changes. The permutations for these are:

$$\binom{M-1}{r-1}\binom{N-1}{r-1}\tau^k\left(\frac{\rho}{\tau}\right)^{2r} \qquad (6)$$

where $r \leq \min(M,N)$.

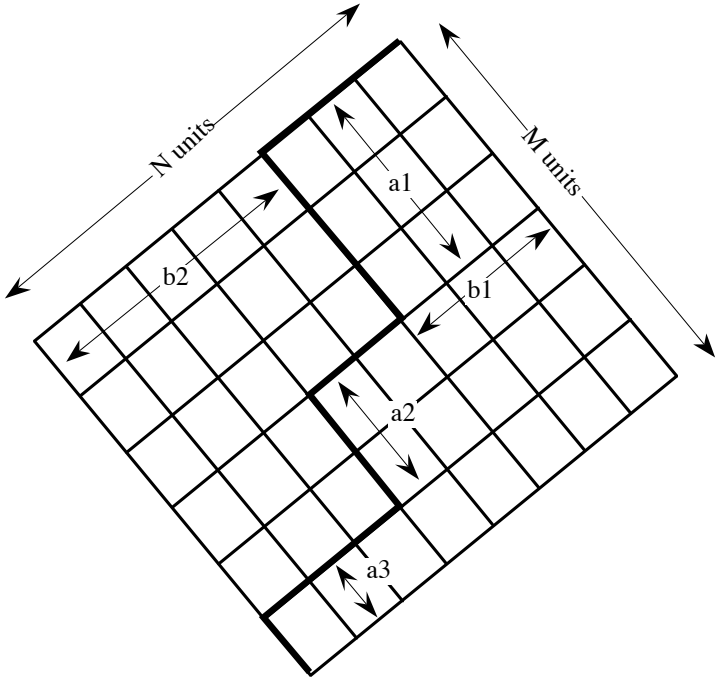

Figure 8

The final case (figure 9) has a sequence $b_1, a_1, b_2, a_2, b_3, a_3$ with 5 changes (this includes the turn at the entry point). So, in general we have a sequence $[b_1, a_1, b_2, a_2, \ldots, b_{r-1}, a_r]$ with (2r-1) changes. The corresponding permutations are:

$$\binom{M-1}{r-1}\binom{N-1}{r-2}\tau^k\left(\frac{\rho}{\tau}\right)^{2r-1} \qquad (7)$$

where $r \leq \min(M+1,N)$.

This approach can provide all contributions inside the extremes τ^k at (x+k) and $\rho\tau^{k-1}$ at (x-k)

For the purpose of using this to predict the contributions at any position due to $\rho^a\tau^{k-a}$ we proceed as follows: Let us imagine that we were interested in the components of $\rho^4\tau^4$ at every possible location at k = 8. That is the power of 4 is even, so we are only interested in the even contributors as defined in the Chardaire method. This can be achieved with 2r = 4 where r = 2 or with 2r - 2 = 4 with r = 3

Thus the contributions of the form $\binom{M-1}{r-1}\binom{N-1}{r-1}\rho^{2r}\tau^{8-2r}$ (r = 2) only have values at (N,M) values of (5,3), (4,4), (3,5) and (2,6). These are shown in bold at the bottom of figure 10.

The contributions of the form $\binom{M-1}{r-1}\binom{N-1}{r-2}\rho^{2r-2}\tau^{8-2r+2}$ (r = 3) only have values at (N,M) values of (6,2), (5,3), (4,4), (3,5) and (2,6). These are also shown in the diagram. The sum of these contributions for each valid position is 5 at (x-4), 12 at (x-2), 18 at (x), 20 at (x+2) and 15 at (x+4) and this is precisely what has been obtained above using other methods. Thus this adaptation of the Chardaire method seems to be a usable method for determining the number of components of any power produce $\rho^a\tau^{k-a}$ for every possible position at iteration, k.

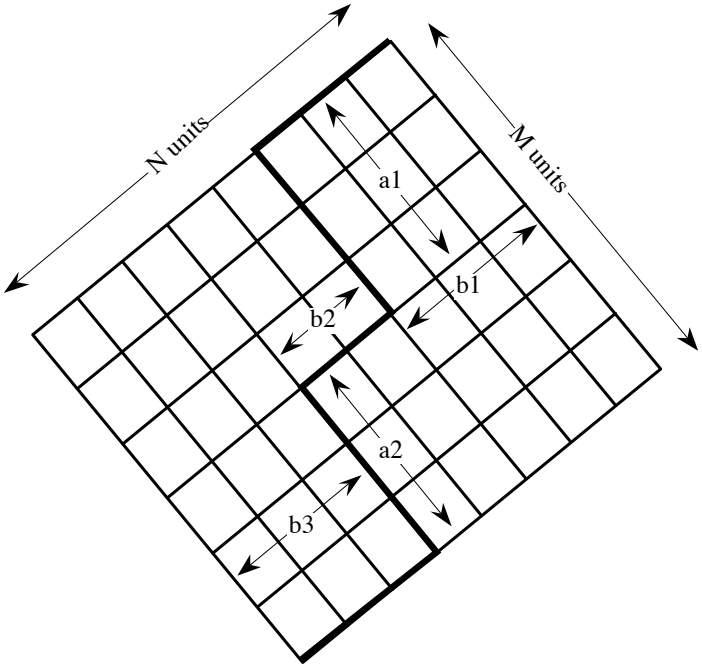

Figure 9

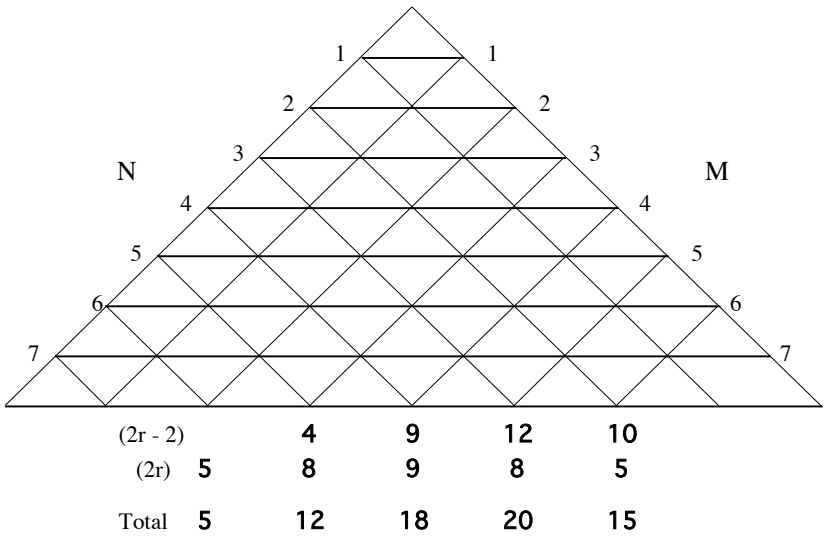

Figure 10

The calculation of variance

The Chardaire method was now used to calculate the population P(x,k) the population at every point following a single unit-magnitude injection from the left. The position of every occupied point at time k and its population were used to calculate variance. When this was first done a minor mistake was made. It was assumed that there was unit distance between occupied cells. Thus, at k = 2, 4, 6 . . . (the distance was $k\Delta x$). In fact there is a distance $2\Delta x$ between occupied cells in a TLM link-line model. For k = 1, 3, 5, . . . it was assumed that distances were separated by an additional $\Delta x/2$. It was noted that if τ was replaced by $(1-\rho)$ throughout and if Maple was allowed to simplify and collect the expressions in powers of r then the outcome seemed to constitute a polynomial of the form:

$$\sigma^2(k) = a_0 - a_1\rho + a_2\rho^2 - a_3\rho^3 + a_4\rho^4 - a_5\rho^5 \ldots \quad (8)$$

The first few terms are shown below:

k	a_0	a_1	a_2	a_3	a_4	a_5	a_6	a_7
2	4	4	-	-	-	-	-	-
3	9	16	8	-	-	-	-	-
4	16	40	40	16	-	-	-	-
5	25	80	120	96	32	-	-	-
6	36	140	280	336	224	64	-	-
7	49	224	560	896	896	512	128	-
8	64	336	1008	2004	2688	2312	1152	256

Considerable time was spent trying to identify the sequences which the coefficients described. Some were easy. The first term, $a_0 = k^2$. The k-th term (a_k) is always 2^k.

Further inspection shows that for all terms greater than a_1 we can use a recurrence relationship to write any polynomial coefficient, $a_j(k)$:

$$a_j(k) = 2*a_{j-1}(k-1) + a_j(k-1)$$

Thus at k = 6 we have $a_3(k) = 2*a_2(5) + a_3(5) = 2*120 + 96 = 336$

This proved quite useful in working backwards to identify the nature of the components and in one avenue of investigation every a_j term was replaced by a polynomial expression in terms of k. It was also noted that the results could be represented by superimposed Pascal triangles and that there was a difference, depending on whether k was odd or even. In early February 2000, with the help of J.H. Conway and R. Guy *The Book of Numbers* it was realised that each of the polynomial coefficients could be represented in terms of C(a,b), where C(7,4) = (7*6*5*4)/(1*2*3*4) = 35.

k	a_0	a_1	a_2	a_3	a_4
2	2^2	$2^2C(3,3)$	-	-	-
3	3^2	$2^2C(4,3)$	$2^3C(4,4)$	-	-
4	4^2	$2^2C(5,3)$	$2^3C(5,4)$	$2^4C(5,5)$	-
5	5^2	$2^2C(6,3)$	$2^3C(6,4)$	$2^4C(6,5)$	$2^5C(6,6)$

This led to the conclusion that $a_j(k) = 2^{j+1}C(k+1,j+2)$, so that instead of

$\sigma^2(k) = a_0 - a_1\rho + a_2\rho^2 - a_3\rho^3 + a_4\rho^4 - a_5\rho^5 + a_0\rho^6 + \ldots$

we can write:

$$\sigma^2(k) = k^2 - 2^2C(k+1,3)\rho + 2^3C(k+1,4)\rho^2 - 2^4C(k+1,5)\rho^3 + \ldots \quad (9)$$

This reduces to $\sigma^2(k) = k^2 + \sum_{j=1}^{k-1}(-\rho)^j 2^{j+1}C(k+1,j+2)$ (10)

but since $k^2 = 2C(k+1,2) - k$ then this reduces to

$$\sigma^2(k) = k^2 + (-\rho)^j \sum_{j=0}^{k-1} 2^{j+1}C(k+1,j+2) \quad (11)$$

Chardaire has supplied a generator function for this expression:

$$\sigma^2(k) = \frac{1}{2\rho^2}\left[(1-2\rho)^{k+1} - 1 + 2(k+1)\rho\right] - k \qquad (12)$$

This can be re-presented in terms of ρ and τ. Alternatively, the observed expression for variance in link-line TLM networks can be presented in terms of only one parameter.

$$\sigma^2(\mathrm{k}) = \frac{\tau}{\rho}\mathrm{k} + \frac{1}{2} - \frac{\tau}{\rho}\left[1 - \frac{\tau}{2\rho}\right] \qquad (13)$$

A formal analysis has now been undertaken where the population P(x,k) is treated as a discrete probability distribution where we calculate the expectation and variance. The result of this is a rigorously proven expression [4]:

$$\sigma^2(k) = \frac{\tau}{\rho}k - \frac{\tau-\rho}{2\rho^2} + \frac{(\tau-\rho)^{k+1}}{2\rho^2} \qquad (14)$$

Extension to two, three and further dimensions

The brute-force method that was described in the early part of this paper becomes almost impossible when the treatment is extended beyond one-dimension. Even the derivation of the local population is difficult enough. Accordingly, the generating function approach due to Chardaire has been used throughout and has provided a comparison between link-line and link-resistor nodes that will be described elsewhere. The variance in two-dimensions is given as

$$\sigma^2(k) = \frac{\tau}{2\rho}k - \frac{\tau^2}{4\rho^2} + \frac{\tau^2(\tau-\rho)^k}{4\rho^2} \qquad (15)$$

and we have demonstrated rigorously that the general form of this expression for n-dimensions is

$$\sigma_n^2(k) = \frac{\tau}{n\rho}k - \frac{\tau^2}{2n\rho^2} + \frac{\tau^2(\tau-\rho)^k}{2n\rho^2} \qquad (16)$$

In all cases we believe that the first term corresponds with the analytical solution for Gaussian diffusion in the appropriate dimension and we suggest that the constant term and the power term are due to the errors that are inherent in the way in which TLM approximates the diffusion equation.

References

1 D. de Cogan, *Transmission Line Matrix (TLM) techniques for diffusion applications* Gordon and Breach 1998 (ISBN 90 5699 129 9)

2 S.J. Cox, (unpublished work)

3 D. de Cogan, *Some observations on spurious effects in Numerical Models* International Journal of Mathematical Algorithms **1**(2) (1999) 153 - 163

4 P. Chardaire & D. de Cogan, *Variance inTLM models for diffusion (part I one-dimensional treatment* (to appear in International Journal of Numerical Modelling)

5 D. de Cogan and A. de Cogan, *Applied numerical modelling for Engineers*, OUP 1997